forests

MDPI

Article

TiO_2-WO_3 Loaded onto Wood Surface for Photocatalytic Degradation of Formaldehyde

Song Li [1,2,†], Zequn Li [2,†], Luming Li [2], Xiangdong Dai [1,*], Meiling Chen [3,*] and Wenkai Zhu [2,*]

[1] College of Furniture and Art Design, Central South University of Forestry and Technology, Changsha 410004, China
[2] College of Chemistry and Materials Engineering, Zhejiang A & F University, Hangzhou 311300, China
[3] Jiangsu Co-Innovation Center of Efficient Processing and Utilization of Forest Resources, College of Materials Science and Engineering, Nanjing Forestry University, Nanjing 210037, China
* Correspondence: daidxd@163.com (X.D.); meiling_chen@njfu.edu.cn (M.C.); wenkai0814@zafu.edu.cn (W.Z.)
† These authors contributed equally to this work.

Abstract: In this work, a facile method was adopted to prepare TiO_2-WO_3 loaded onto a wood surface by a two-step hydrothermal method. The as-prepared wood composite material can be used as a photocatalyst under UV irradiation for the photodegradation of formaldehyde. Related tests showed that TiO_2-WO_3 nano-architectonic materials with spherical particles loaded onto the wood substratewere mainly caused by self-photodegradation of formaldehyde. The TiO_2-WO_3 nanostructured material firmly adheres to the wood substrate through electrostatic and hydrogen bonding interactions. Meanwhile, the appearance of the new chemical bond Ti-O-W indicates the successful loading of TiO_2-WO_3 onto the wood surface. The photodegradation rate was measured and it was confirmed that the highest photodegradation performance of the modified wood was achieved at a molar ratio of 5:1 of TiO_2 to WO_3. This work provides a new strategy for the preparing of novel photocatalysts based on wood substrate. Moreover, the wood loaded with TiO_2-WO_3 is a promising candidate for indoor formaldehyde treatment in practical applications.

Keywords: wood substrate; TiO_2; WO_3; photocatalytic activity; formaldehyde

Citation: Li, S.; Li, Z.; Li, L.; Dai, X.; Chen, M.; Zhu, W. TiO_2-WO_3 Loaded onto Wood Surface for Photocatalytic Degradation of Formaldehyde. *Forests* **2023**, *14*, 503. https://doi.org/10.3390/f14030503

Academic Editor: Nadir Ayrilmis

Received: 6 January 2023
Revised: 1 March 2023
Accepted: 1 March 2023
Published: 3 March 2023

1. Introduction

Adhesives with formaldehyde as the main component are widely used in producing house decoration materials and furniture. In addition, they will release formaldehyde into the air, affecting human health [1,2]. With the improvement in people's concept of health and environmental protection, increasingly more people are aware of the harm of formaldehyde. Therefore, the removal of indoor formaldehyde has important practical significance. The commonly used methods for the elimination of formaldehyde mainly include plasma catalytic degradation, electrocatalytic oxidation degradation, physical absorption treatment, plant purification, and photocatalytic degradation [3–6]. It includes not only the physical method but also the chemical method. The photocatalytic degradation materials developed in recent years have shown great potential in the degradation of free formaldehyde in indoor air [7–9]. However, recycling these powdery semiconductor photocatalysts has become an essential issue in the practical application process.

The material most closely related to the human living environment is wood. It has a high strength-to-weight ratio, low density, easy processing, an excellent thermal-electrical insulation, but also outstanding acoustic properties and other advantages [10–13]. In addition, wood is also a superior biomass carrier and has a naturally porous structure. In interior decoration and furniture-making materials, wood is also an inevitable consumable. Photocatalytic technology only needs to be illuminated in nature or indoors to cause chemical changes, and it is harmless to humans and the environment, which is a "green" process [14]. Therefore, it is feasible to carry out composite modification on wood and

apply it to the photocatalytic degradation of formaldehyde. The composite modification of wood and inorganic nanomaterials makes it recyclable and formaldehyde degradable, becoming a research hotspot in this field in recent years [15–17].

The TiO_2 semiconductor with a band gap of 3.2 eV is a promising photocatalyst. Because of its non-toxic, harmless, corrosion resistance, environmental protection, strong photocatalytic oxidation ability, and high stability, it is widely used in the photodegradation of water or gaseous toxic organic pollutants [18–20]. In the photodegradation of toxic pollutants by TiO_2, the whole process is simple and environmentally friendly. It takes place at normal temperature and pressure, and the reaction products are usually CO_2 and water. Since Fujishima et al. [21] invented photocatalytic decomposition on TiO_2 single crystal electrodes in 1972, they have attracted extensive attention from many researchers. It has attracted scientists from different research fields to carry out significant research on TiO_2 preparation and photocatalytic performance. However, TiO_2 has a large band gap, which makes the solar energy utilization rate low. The photocatalytic performance of TiO_2 can be improved by using methods such as doping metal oxides, doping non-metal oxides, co-doping metal and non-metal oxides, semiconductor compounding, and photocatalyst photosensitization [22–26]. Related studies showed that the photocatalytic efficiency of TiO_2-WO_3 composite nanomaterials prepared by the sol-gel method and temperature-controlled calcination method could reach 94.8% for acid red B [27]. WO_3 has a narrower band gap, a wider light absorption range, and a more efficient use of sunlight [28]. Therefore, compounding TiO_2 and WO_3 to improve the photocatalytic degradation efficiency of formaldehyde has aroused extensive research in the academic community.

As one of the best photocatalysts, WO_3 has a small band gap and a large light absorption range. Making more efficient use of visible light accounts for nearly half of the sun's radiation [29,30]. However, it is difficult to obtain stable photocatalytic performance of pure WO_3 due to its defects, such as easy photo corrosion. Moreover, TiO_2 is a catalyst with many advantages, but its small absorption range is the main application limitation. WO_3 can improve this limitation, so materials doped with WO_3 have also become a current research hotspot [31,32]. On the other hand, wood is an outstanding carrier, which has a natural porous structure, a large number of capillaries inside, and a large specific surface area. Therefore, it is of great significance to explore a simple and effective method to obtain a composite catalyst with a better catalytic effect on the surface of TiO_2 and WO_3 composite wood.

In this study, wood surfaces loaded with TiO_2-WO_3 composites with different composite proportions were prepared by a two-step low temperature hydrothermal method. Meanwhile, the crystallinity and morphology characteristics were discussed, and its growth on the wood surface was studied. Furthermore, the photocatalytic mechanism of formaldehyde degradation was discussed by studying its photocatalytic performance. The properties of photocatalytic formaldehyde were also studied. The purpose of this study was to obtain wood loaded with TiO_2-WO_3 composites with high photocatalytic performance and to investigate their application to degrade the free formaldehyde released indoors.

2. Materials and Methods

2.1. Materials

Poplar wood samples (Populus sp., 8 × 8 × 2 mm^3, length × width × high, moisture content was 10.33%) were supplied by Dehua Bunny Decoration New Materials Co., Ltd. (Huzhou, China), which was sapwood with eight annual rings. Ammonium hexafluorotitanate(IV) ($(NH_4)_2TiF_6$, ≥99%), boric acid (H_3BO_3), and tungsten(VI) chloride ($WCl_6 \cdot 6H_2O$, ≥99.9%) were purchased from Shanghai Boyle Chemical Co., Ltd. (Shanghai, China). Ethanol absolute (C_2H_5OH, ≥99.9%), and hydrochloric acid (HCl, ≥99.9%) were bought from Nanjing Lisheng Chemical Company (Nanjing, China). All reagents are analytical pure grade and can be used directly without secondary purification. Moreover, deionized water was used in all experiments.

2.2. Preparation of TiO_2 Loaded onto Wood

Briefly, $(NH_4)_2TiF_6$ (0.989 g) and H3BO3 (0.927 g) were mixed with a deionized water solution (600 mL) and stirred for two h at room temperature. After that, adjusted the pH value to 3 with 0.3 mol/L HCl solution. Subsequently, the mixed solution was placed in a reaction kettle, and five wood samples were respectively placed and reacted at 70 °C for 5 h. Then, the wood samples were removed and cleaned with deionized water three times (10 min each time). Finally, the samples were placed in a vacuum oven and dried at 45 °C for 24 h. Thus, the samples of TiO2 loaded onto wood were prepared. In addition, each set of experiments was repeated three times to ensure the accuracy of the experiment.

2.3. Preparation of TiO_2-WO_3 Loaded onto Wood

The schematic illustration of the preparation of TiO_2-WO_3 loaded onto wood is shown in Figure 1. Four of the above wood samples and one unreacted wood sample were obtained and sonicated with ethanol. Then, a certain amount of $WCl_6 \cdot 6H_2O$ was dissolved in 100 mL of ethanol solution, placed in the wood sample and stirred magnetically for 2 h at room temperature. Subsequently, after standing and impregnating at room temperature for 24 h, the wood samples were removed and placed in a vacuum-drying oven for 24 h to obtain TiO_2-WO_3 loaded onto wood. The changed amounts of WO_3 in TiO_2-WO_3 can be obtained by controlling the molar ratio of $WCl_6 \cdot 6H_2O$ in the mixed solution. The molar ratios of WO_3 and TiO_2 were set as 1:0, 1:1, 1:3, and 1:5. The as-prepared wood samples with the molar ratio of WO_3 and TiO_2 (1:0, 1:1, 1:3, and 1:5) were labeled as TW1, TW2, TW3, and TW4, respectively (the specific formulation is shown in Table 1). Moreover, the unmodified blank control sample was named TW0.

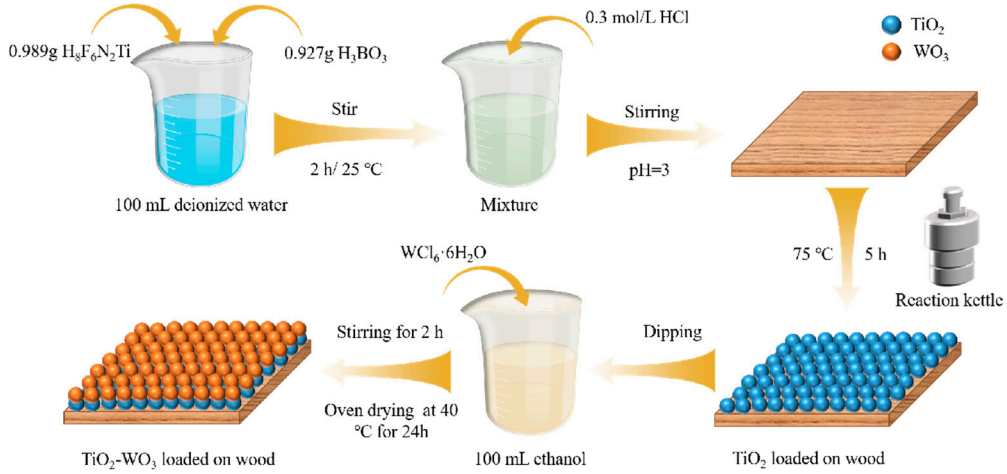

Figure 1. Schematic illustration of the preparation of TiO_2-WO_3 loaded onto wood.

Table 1. The molar ratio of WO_3 and TiO_2 in as-prepared wood samples.

Samples / Molar Ratio	TW0	TW1	TW2	TW3	TW4
WO_3:TiO_2	0:0	1:0	1:1	1:3	1:5

2.4. Characterization

The surface morphology of the wood substrate before and after being loaded by TiO_2-WO_3 was investigated by scanning electron microscopy (SEM, Quant 200, FEI Company, Hillsboro, OR, USA). The crystalline structures of the samples were measured by X-ray diffraction (XRD, D/MAX 2200, Rigaku, Japan). The XRD was conducted with Cu-Kα radiation at 40 kV and 30 mA with a step rate of 4°/min ranging from 10° to 80°. The chemical functional groups change of the samples was carried out using a attenuated total reflection Fourier Transformed Infrared Spectrometer (ATR-FTIR, Magna-IR 560, Nicolet

Bankshares, Inc., Green Bay, WI, USA), which was conducted in the range of 400~4000 cm^{-1} with a resolution of 4 cm^{-1}. All spectra were recorded at room temperature and there was a drying system which could prevent atmospheric moisture from interfering with the spectrum.

2.5. Formaldehyde Degradation Performance Test

The photocatalytic formaldehyde degradation performance of the as-prepared samples was tested at room temperature, and the schematic diagram of the device is shown in Figure 2. Moreover, three samples were made of each type of TW1–TW4 and all samples were studied in the photocatalytic degradation experiment. The average of the three test results was obtained as the final test result. The whole tests were carried out in a cylindrical glass caulk with an expanded volume of 0.1 m^3. The LED light (λ max = 458 nm, emission intensity of approximately 3.6 mW/cm^2) was fixed at the center of the opening and used to simulate visible light. The desired dose of formaldehyde was added to the tamponade, and the fan was maintained for 30 min to obtain an adsorption and desorption balance. After the adsorption equilibrium, the initial concentration of formaldehyde in the obturator can be determined by Formaldemeter (LB-HD05, China). Subsequently, the LED light was turned on to illuminate the sample, and each set of degradation experiments was continued under the LED light for 6 h. The degradation efficiency of formaldehyde was estimated by the following formula:

$$D(\%) = \frac{C_0 - C}{C_0} \times 100\% \quad (1)$$

where C_0 is the initial concentration of the formaldehyde, and C represents the measured formaldehyde concentration.

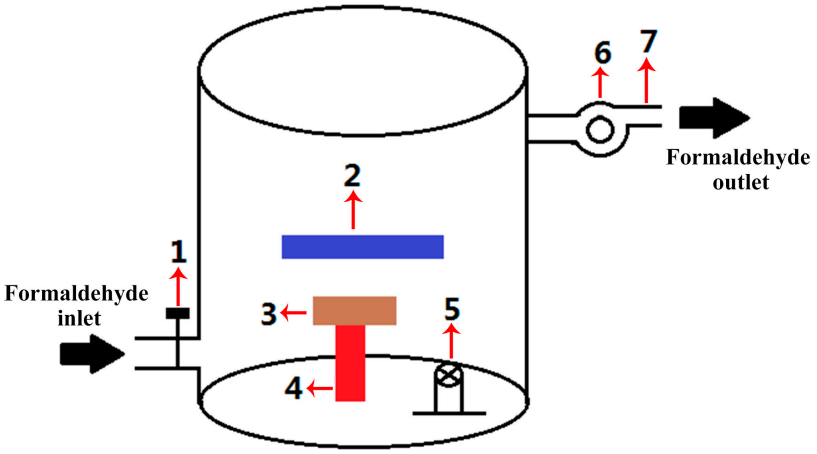

Figure 2. Schematic diagram of the experimental setup for photocatalytic degradation of formaldehyde. (1) Speedometer; (2) LED light; (3) wood sample; (4) support cantilever; (5) fan; (6) variable frequency suction fan; (7) formal wind speed.

3. Results and Discussion

3.1. Morphological Characterizations

Figure 3 displays the SEM images of the as-prepared wood samples loaded with different proportions of TiO_2-WO_3. Figure 3a presents the microtopography of the surface of the TW1 samples; it can be clearly seen from the figure that tiny particles grow on the surface of the modified wood sample and cover the surface. These tiny particles are roughly spherical with many edges and corners. Figure 3b,c are the surface morphologies of TW2 and TW3. As shown in the figures, the surface of the samples is covered with small spherical particles, and some of them are agglomerated together. Moreover, the agglomeration phenomenon on the surface of the sample was more severe than that of the TW1 sample, and the particle size also increased. Figure 3d displays the SEM image

of TW4, and the growth conditions of the nanoparticles on the surface are also similar to those in Figure 3a–c, but the particles are denser. However, the particle size is smaller than that in Figure 3a–c. Based on the above analysis, it can be inferred that the average particle size of TiO_2 particles on the wood surface increases gradually with the increase in WO_3 content. Furthermore, the agglomeration effect will also increase, but the addition of WO_3 has little effect on the morphology of the product. The successful loading of TiO_2-WO_3 nanoparticles on the wood sample makes the wood surface form a dense metal oxide film structure, which is beneficial to improve the photocatalytic formaldehyde degradation performance of wood. More importantly, the surface microstructure of the wood did not change significantly after irradiation, suggesting that the surface-loaded nanoparticles only acted as catalysts.

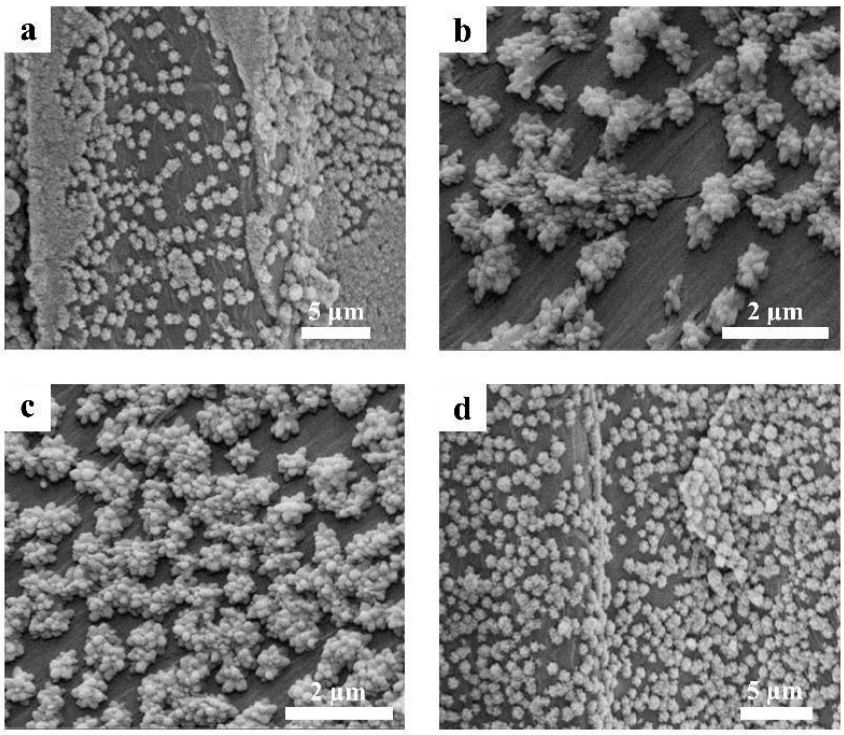

Figure 3. SEM images of TW1 (**a**), TW2 (**b**), TW3 (**c**), and TW4 (**d**).

3.2. XRD Analysis

The crystal structure of the wood sample before and after the modification can be analyzed by XRD patterns, as shown in Figure 4. The diffraction peaks present at 16° and 22.5° belong to the (101) and (002) crystal surfaces of the cellulose in the wood [33]. The diffraction peaks of the wood composite loaded with TiO_2-WO_3 at 25.3°, 38.0°, 47.6°, 54.3°, and 64.5° are consistent with the (101), (004), (200), (105), and (204) crystal surfaces in TiO_2 [34,35], respectively. Therefore, the TiO_2 loaded onto the surface of the wood samples corresponds to rutile phase TiO_2 and anatase phase TiO_2. Meanwhile, the results also showed that TiO_2 was successfully loaded onto the wood surface. Moreover, the modified wood samples showed diffraction characteristic peaks at 2 θ of 22.6°, 25.8°, 30°, and 34.5°, which matched with the (001), (110), (200), and (201) crystal planes in WO_3, respectively. It is consistent with the WO_3 triclinic phase (JCPDS No. 32-1295), which indicates that WO_3 particles were successfully loaded onto the surface of the samples [36]. In the XRD spectra of samples TW1, TW2, TW3, and TW4, some obvious TiO_2 and WO_3 characteristic diffraction peaks also appeared. With the increase in the concentration of TiO_2 in TiO_3-WO_3, the characteristic peak of TiO_2 in the composite sample is also enhanced. This indicates that different ratios of TiO_2 and WO_3 can be successfully loaded onto the surface of wood samples.

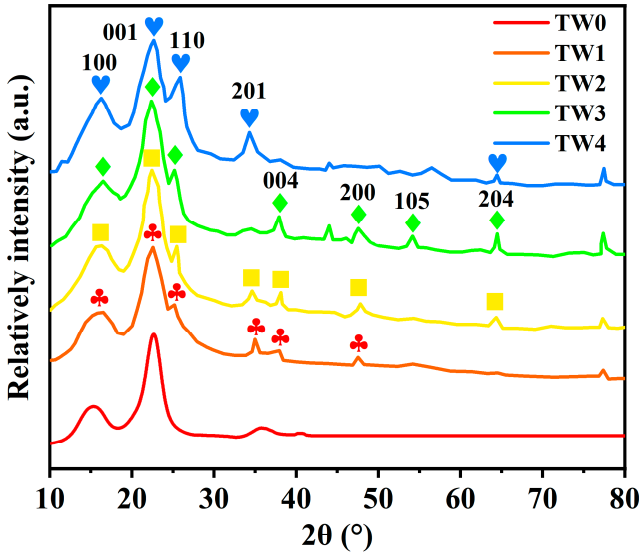

Figure 4. XRD patterns of TW0, TW1, TW2, TW3, and TW4.

3.3. ATR-FTIR Analysis

ATR-FTIR is a conventional test method for analyzing the functional groups, chemical structures, and binding mechanisms of samples. Figure 5 shows the spectra of the wood modified by TiO_2-WO_3. It can be clearly seen from Figure 5a that the vibrational absorption peak at 3398 cm^{-1} is caused by the hydrogen bond of the hydroxyl group (-OH) in wood or the stretching vibration of O-H in water [37]. This peak was enhanced after the modification, which may result from the hydrogen bond generated from the reaction of TiO_2 or WO_3 with the hydroxyl group on the wood surface. The absorption peak at a wavelength of 2927 cm^{-1} is caused by the asymmetric stretching vibration of the C-H bond in the long-chain group -CH_3 in the wood [38]. The characteristic absorption peaks occurring at 1060 cm^{-1} and 1629 cm^{-1} are caused by C-O and C=O stretching vibrations in wood, respectively. The appearance of the above characteristic peaks showed that the wood did not destroy its unique structure of wood during the experiment [39]. Moreover, it can be seen from Figure 5b that TW1, TW2, TW3, and TW4 have W-O stretching vibration peaks at 820 cm^{-1} and 890 cm^{-1}, which were not found in the TW0 absorption curve of the samples. Meanwhile, the Ti-O vibration peak appeared at the wavenumber of 641 cm^{-1}, but it was not found in the spectrum of TW0. The spectrum indicated that the composite products of TiO_2-WO_3 appeared in TW1, TW2, TW3, and TW4, and were well loaded onto the wood surface. Meanwhile, the spectra of the irradiated wood did not change.

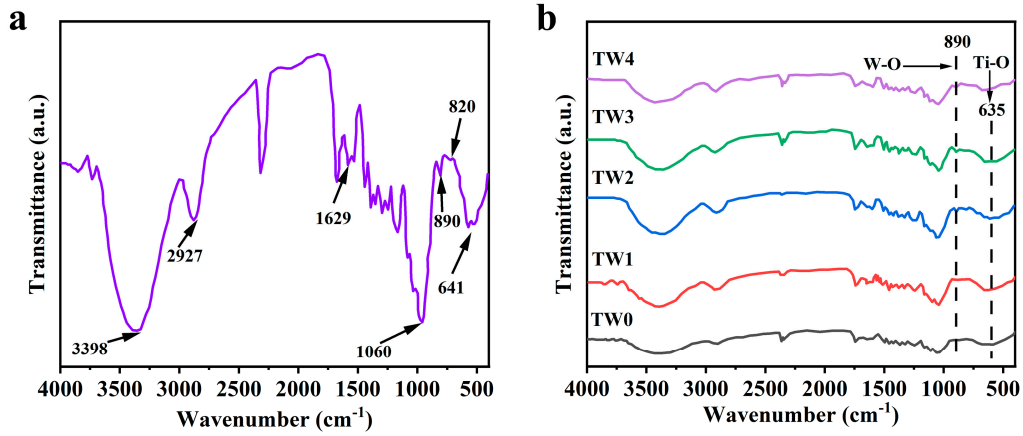

Figure 5. (**a**) ATR-FTIR spectra of TW1. (**b**) ATR-FTIR spectra of the wood before and after modification by TiO_2-WO_3.

3.4. Photocatalytic Degradation Performance

In order to explore the effect of wood samples modified with different TiO_2-WO_3 molar ratios on the performance of the photocatalytic degradation of formaldehyde, the degradation performance of all samples under UV light was tested, and the results are shown in Figure 6a. The concentration of formaldehyde was set to 2.5 mg/m^3 during the test. The photocatalytic degradation efficiency of formaldehyde in untreated wood samples was close to zero, indicating that there was almost no degradation of formaldehyde. The photocatalytic efficiency of the TW1 sample under visible light irradiation was low, which was about 37.03%, while the samples of TW2, TW3 and TW4 showed higher photocatalytic degradation performance, and the photocatalytic efficiency of TW2, TW3, and TW4 was 73.13%, 92.10%, and 97.86%, respectively. The results showed that the photocatalytic properties of the as-prepared wood products improved rapidly with the increasing amount of TiO_2. Compared with other samples, TW4 had the best photocatalytic performance with a degradation rate of about 98%. There may be several reasons for the above phenomenon. Firstly, TiO_2 can deposit the WO_3 band with a higher donor value than the initial value on the wood substrate, which improves the absorption efficiency of visible light irradiation [40]. With increasing TiO_2 content, the distance between the donor level and the valence band becomes greater. Therefore, a large number of electrons are generated under visible light excitation, which is conducive to enhancing photocatalytic degradation. Secondly, when the content of TiO_2 is lower than its proper molar ratio, TiO_2 mainly occurs on the surface area of the sample to hunt and convert electrons and holes, which will inhibit the recombination of photoexcited holes and electrons. The photoexcited electrons and holes of the modified wood samples will photodegrade formaldehyde into CO_2 and H_2O.

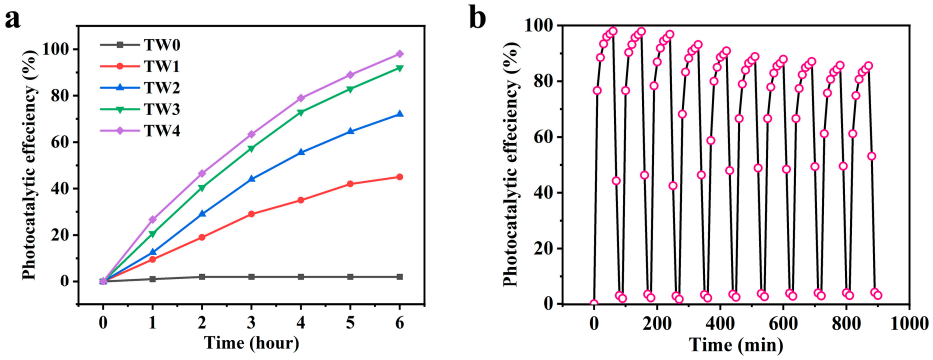

Figure 6. (**a**) Photocatalytic efficiency of formaldehyde of all samples. (**b**) Ten cycles of the photocatalytic efficiency of TW4 for formaldehyde.

In addition, the reusability of TW4 samples as typical representatives was studied, as shown in Figure 6b. In order to evaluate the recyclability of the as-prepared wood sample, 10 recycling tests were carried out on the degradation of formaldehyde. Obviously, the TW4 sample can still maintain excellent photocatalytic performance after 10 photocatalytic cycles, with an efficiency of more than 85%. The decrease in degradation rate was mainly due to the slight leaching of TiO_2-WO_3 nanoparticles in each recovery experiment. Therefore, the wood surface-loaded TiO_2-WO_3 composite material has a certain application potential as a photocatalyst in the removal of indoor formaldehyde pollutants.

3.5. Mechanism of Photocatalytic Degradation of Formaldehyde

Based on the above photocatalytic results, we constructed the potential energy diagram and formaldehyde degradation mechanism diagram of the wood surface loaded with TiO_2-WO_3 composite material, as shown in Figure 7. When the treated wood is irradiated by ultraviolet light, the conduction bands (CB) of TiO_2 and WO_3 both generate excited electrons. Due to the potential difference, the photogenerated electrons in WO_3 can easily move to the CB of TiO_2. Therefore, electron transfer will reduce the chance of recombination with

the holes formed in the valence bands (VB) of the TiO_2 and WO_3. The holes migrate directly from TiO_2 to WO_3 and then to the wood substrate interface. Thus, reduced recombination results in enhanced photoactivity. According to the previous references [41,42], Figure 7 and Equations (2)–(8) showed the photocatalytic degradation reaction of formaldehyde, where hv, h^+, e^-, •OH, and $•O_2^-$ represent light energy, holes, electron, hydroxyl radicals, and superoxide radicals.

$$TiO_2 + hv \rightarrow TiO_2(h^+ + e^-) \quad (2)$$

$$WO_3 + hv \rightarrow WO_3(h^+ + e^-) \quad (3)$$

$$h^+ + H_2O \rightarrow {}^{\bullet}OH + H^+ \quad (4)$$

$$Ti^{4+} + e^- \rightarrow Ti^{3+} \quad (5)$$

$$Ti^{3+} + O_2 \rightarrow Ti^{4+} + {}^{\bullet}O_2^- \quad (6)$$

$$HCHO + {}^{\bullet}OH \rightarrow {}^{\bullet}CHO + H_2O \quad (7)$$

$${}^{\bullet}CHO + {}^{\bullet}OH \rightarrow HCOOH \quad (8)$$

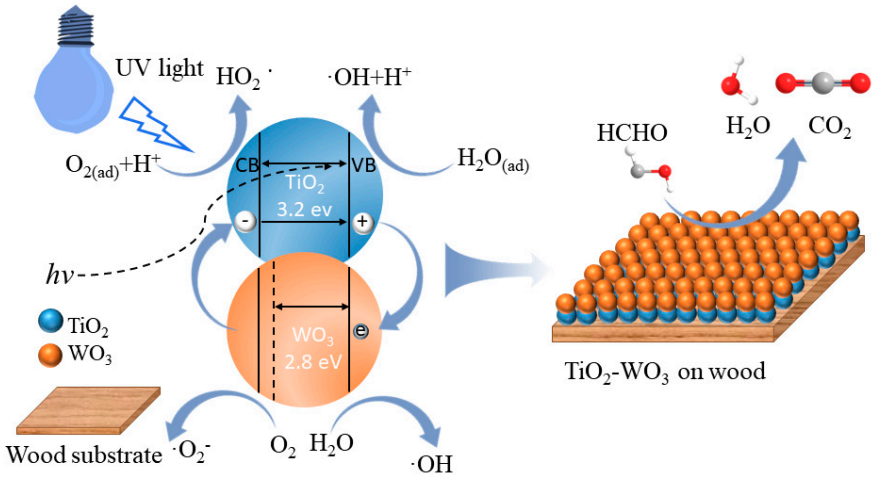

Figure 7. Photocatalytic mechanism schematic diagrams of the wood loaded with TiO_2-WO_3 composite material.

Obviously, the electrons in the VB of TiO_2 are excited to the CB of TiO_2 under UV irradiation. It shifted from the CB of TiO_2 to WO_3 due to the lower CB of WO_3. The holes left in the VB of WO_3 can move to the valence electrons of TiO_2, which is beneficial to the electron/hole separation. Therefore, the photocatalytic degradation efficiency of the sample was improved. The free radicals (•OH and $•O_2^-$) produced by catalysis can efficiently degrade formaldehyde to produce carbon dioxide and water.

4. Conclusions

In this work, we have presented TiO_2-WO_3 loaded onto a wood substrate fabricated by a two-step hydrothermal method. The wood served as biomass substrates to prepare the TiO_2-WO_3 photocatalysts with nano-architectonic spherical particles. The wood loaded with TiO_2-WO_3 composite material was characterized via various techniques and the photocatalytic degradation property was tested by degrading formaldehyde. The as-prepared wood sample exhibits higher potential for application as a photocatalyst for the degradation of formaldehyde, and the photocatalytic degradation efficiency can reach 98%. These studies indicated that TiO_2-WO_3 successfully loaded onto the wood surface concern only the surface, which could provide more active sites for photocatalysis. Furthermore, the as-prepared wood can still maintain more than 80% formaldehyde photodegradation efficiency after 10 times of recycling. Additionally, the photocatalytic degradation mechanism of formaldehyde shows that the loaded TiO_2-WO_3 reduces the recombination probability

of photoexcited carriers and increases the transport of charges. This work will provide a new strategy for preparing novel wood-based photocatalysts with photocatalytic formaldehyde degradation performance. Moreover, it has practical significance to apply it to the degradation of indoor formaldehyde.

Author Contributions: Conceptualization, S.L., X.D. and W.Z.; methodology, Z.L. and M.C.; software, M.C. and S.L.; validation, S.L., M.C. and W.Z.; formal analysis, X.D., S.L. and L.L.; investigation, Z.L.; resources, M.C.; data curation, S.L. and L.L.; writing—original draft preparation, S.L., W.Z. and M.C.; writing—review and editing, S.L., M.C. and W.Z.; visualization, X.D.; supervision, S.L. and X.D.; project administration, Z.L. and M.C.; funding acquisition, S.L. All authors have read and agreed to the published version of the manuscript.

Funding: This research was funded by Nanjing Science and Technology Innovation Project for Overseas Students, the Research and Development Funding of Zhejiang A & F University (2022LFR076), the Project Funded by the Natural Science Foundation of Jiangsu Province of China (BK20201072), the National Natural Science Foundation of China (22078123, 32071687), and the Natural Science Foundation of the Higher Education Institutions of Jiangsu Provience (19KJB22006).

Institutional Review Board Statement: Not applicable.

Informed Consent Statement: Not applicable.

Data Availability Statement: The data that support the findings of this study are available from the corresponding author, S.L., upon reasonable request.

Acknowledgments: We would like to thank other members of our groups for helping us prepare for the samples. The advanced analysis and testing center of Zhejiang A & F University is acknowledged.

Conflicts of Interest: The authors declare no conflict of interest.

References

1. Malayeri, M.; Bahri, M.; Haghighat, F.; Shah, A. Impact of air distribution on indoor formaldehyde abatement with/without passive removal material: A CFD modeling. *Build. Environ.* **2022**, *212*, 108792. [CrossRef]
2. Li, X.; Shi, R.; Li, J. Effect of clay on properties of melamine-urea-formaldehyde resin. *J. For. Eng.* **2022**, *7*, 78–83.
3. Wang, X.; Hong, S.; Lian, H.; Zhan, X.; Cheng, M.; Huang, Z.; Manzo, M.; Cai, L.; Nadda, A.; Van Le, Q. Photocatalytic degradation of surface-coated tourmaline-titanium dioxide for self-cleaning of formaldehyde emitted from furniture. *J. Hazard. Mater.* **2021**, *420*, 126565. [CrossRef]
4. Soni, V.; Goel, V.; Singh, P.; Garg, A. Abatement of formaldehyde with photocatalytic and catalytic oxidation: A review. *Int. J. Chem. React. Eng.* **2021**, *19*, 1–29. [CrossRef]
5. Sahrin, N.T.; Nawaz, R.; Chong, F.K.; Lee, S.L.; Wirzal, M.D.H. Current perspectives of anodized TiO2 nanotubes towards photodegradation of formaldehyde: A short review. *Environ. Technol. Innov.* **2021**, *22*, 101418. [CrossRef]
6. Zhu, W.; Kim, D.; Han, M.; Jang, J.; Choi, H.; Kwon, G.; Jeon, Y.; Ryu, D.Y.; Lim, S.-H.; You, J.; et al. Fibrous Cellulose Nanoarchitectonics on N-doped Carbon-based Metal-Free Catalytic Nanofilter for Highly Efficient Advanced Oxidation Process. *Chem. Eng. J.* **2023**, *460*, 141593. [CrossRef]
7. Qin, X.; Liu, Y.; Xu, Y.; Wu, L.; Huang, K.; Huang, J.; Wang, W. Effect of microencapsulation of formaldehyde capture agents on formaldehyde emission from veneered panels. *J. For. Eng.* **2020**, *5*, 81–87.
8. Ran, M.; Cui, W.; Li, K.; Chen, L.; Zhang, Y.; Dong, F.; Sun, Y. Light-induced dynamic stability of oxygen vacancies in $BiSbO_4$ for efficient photocatalytic formaldehyde degradation. *Energy Environ. Mater.* **2022**, *5*, 305–312. [CrossRef]
9. Lin, Z.; Shen, W.; Corriou, J.-P.; Chen, X.; Xi, H. Assessment of multiple environmental factors on the adsorptive and photocatalytic removal of gaseous formaldehyde by a nano-TiO_2 colloid: Experimental and simulation studies. *J. Colloid Interface Sci.* **2022**, *608*, 1769–1781. [CrossRef]
10. Wang, J.; Wu, X.; Wang, Y.; Zhao, W.; Zhao, Y.; Zhou, M.; Wu, Y.; Ji, G. Green, Sustainable Architectural Bamboo with High Light Transmission and Excellent Electromagnetic Shielding as a Candidate for Energy-Saving Buildings. *Nano-Micro Lett.* **2023**, *15*, 11. [CrossRef]
11. Grönquist, P.; Wood, D.; Hassani, M.M.; Wittel, F.K.; Menges, A.; Rüggeberg, M. Analysis of hygroscopic self-shaping wood at large scale for curved mass timber structures. *Sci. Adv.* **2019**, *5*, eaax1311. [CrossRef] [PubMed]
12. Gan, W.; Wang, Y.; Xiao, K.; Zhai, M.; Wang, H.; Xie, Y. Research review of energy storage and conversion materials based on wood cell wall functional modification. *J. For. Eng.* **2022**, *7*, 1–12.
13. Hill, C.; Altgen, M.; Rautkari, L. Thermal modification of wood—A review: Chemical changes and hygroscopicity. *J. Mater. Sci.* **2021**, *56*, 6581–6614. [CrossRef]

14. Ijaz, M.; Zafar, M. Titanium dioxide nanostructures as efficient photocatalyst: Progress, challenges and perspective. *Int. J. Energy Res.* **2021**, *45*, 3569–3589. [CrossRef]
15. Wang, J.; Hu, X.; Li, M.; Shao, L.; Zhan, J. Preparation of wood-based yttrium doped TiO_2 film and its photocatalytic properties. *J. For. Eng.* **2021**, *6*, 51–57.
16. Li, Z.; Wang, S.; Wu, J.; Zhou, W. Recent progress in defective TiO_2 photocatalysts for energy and environmental applications. *Renew. Sustain. Energy Rev.* **2022**, *156*, 111980. [CrossRef]
17. Yuan, D.; Liu, Y.; Wang, W.; Gao, L.; Cheng, J. Preparation of titanium dioxide based on poplar template and its application on formaldehyde degradation. *J. For. Eng.* **2020**, *5*, 34–40.
18. Basavarajappa, P.S.; Patil, S.B.; Ganganagappa, N.; Reddy, K.R.; Raghu, A.V.; Reddy, C.V. Recent progress in metal-doped TiO_2, non-metal doped/codoped TiO_2 and TiO_2 nanostructured hybrids for enhanced photocatalysis. *Int. J. Hydrog. Energy* **2020**, *45*, 7764–7778. [CrossRef]
19. Zhu, Y.; Zhu, W.; Li, Z.; Feng, Y.; Qi, W.; Li, S.; Wang, X.; Chen, M. Enhancement of Wood Coating Properties by Adding Silica Sol to UV-Curable Waterborne Acrylics. *Forests* **2023**, *14*, 335. [CrossRef]
20. Guo, Q.; Zhou, C.; Ma, Z.; Yang, X. Fundamentals of TiO_2 photocatalysis: Concepts, mechanisms, and challenges. *Adv. Mater.* **2019**, *31*, 1901997. [CrossRef]
21. Fujishima, A.; Honda, K. Electrochemical photolysis of water at a semiconductor electrode. *Nature* **1972**, *238*, 37–38. [CrossRef] [PubMed]
22. De Oliveira, C.P.M.; Moreira, V.R.; Lebron, Y.A.R.; de Vasconcelos, C.K.B.; Koch, K.; Viana, M.M.; Drewes, J.E.; Amaral, M.C.S. Converting recycled membranes into photocatalytic membranes using greener TiO_2-GRAPHENE oxide nanomaterials. *Chemosphere* **2022**, *306*, 135591. [CrossRef] [PubMed]
23. Lee, R.; Lim, C.; Lee, H.; Kim, S.; Lee, Y.-S. Visible light photocatalytic activity of TiO_2 with carbon-fluorine heteroatoms simultaneously introduced by CF_4 plasma. *Korean J. Chem. Eng.* **2022**, *39*, 3334–3342. [CrossRef]
24. Yu, H.; Zhao, S.; Mao, W.; Faheem, M.; Ding, D.; Chen, L.; Cai, T. Facile synthesis of N-doped TiO_2 and its photocatalytic properties for ciprofloxacin degradation. *Funct. Mater. Lett.* **2022**, *15*, 2250028. [CrossRef]
25. Liu, K.; Kong, F.; Zhu, C.; Jiang, G. Photocatalytic activity of phosphorus and nitrogen co-doped carbon quantum dots/TiO_2 nanosheets. *Nano* **2020**, *15*, 2050151. [CrossRef]
26. Chen, D.; Cheng, Y.; Zhou, N.; Chen, P.; Wang, Y.; Li, K.; Huo, S.; Cheng, P.; Peng, P.; Zhang, R. Photocatalytic degradation of organic pollutants using TiO_2-based photocatalysts: A review. *J. Clean. Prod.* **2020**, *268*, 121725. [CrossRef]
27. Zhang, L.; Qin, M.; Yu, W.; Zhang, Q.; Xie, H.; Sun, Z.; Shao, Q.; Guo, X.; Hao, L.; Zheng, Y. Heterostructured TiO_2/WO_3 nanocomposites for photocatalytic degradation of toluene under visible light. *J. Electrochem. Soc.* **2017**, *164*, H1086. [CrossRef]
28. Samuel, O.; Othman, M.H.D.; Kamaludin, R.; Sinsamphanh, O.; Abdullah, H.; Puteh, M.H.; Kurniawan, T.A. WO_3–based photocatalysts: A review on synthesis, performance enhancement and photocatalytic memory for environmental applications. *Ceram. Int.* **2021**, *48*, 5845–5875. [CrossRef]
29. Tahir, M.; Ali, S.; Rizwan, M. A review on remediation of harmful dyes through visible light-driven WO_3 photocatalytic nanomaterials. *Int. J. Environ. Sci. Technol.* **2019**, *16*, 4975–4988. [CrossRef]
30. Thirumoorthi, G.; Gnanavel, B.; Kalaivani, M.; Ragunathan, A.; Venkatesan, H. Suitability of Iron (Fe)-Doped Tungsten Oxide (WO_3) Nanomaterials for Photocatalytic and Antibacterial Applications. *Int. J. Nanosci.* **2021**, *20*, 2150042. [CrossRef]
31. Karthikeyan, S.; Selvapandiyan, M.; Sasikumar, P.; Parthibavaraman, M.; Nithiyanantham, S.; Srisuvetha, V. Investigation on the properties of vanadium doping WO_3 nanostructures by hydrothermal method. *Mater. Sci. Energy Technol.* **2022**, *5*, 411–415. [CrossRef]
32. Jiang, H.; Li, Y.; Wang, D.; Hong, X.; Liang, B. Recent advances in heteroatom doped graphitic carbon nitride (g-C_3N_4) and g-C_3N_4/metal oxide composite photocatalysts. *Curr. Org. Chem.* **2020**, *24*, 673–693. [CrossRef]
33. Zhu, W.; Zhang, Y.; Wang, X.; Wu, Y.; Han, M.; You, J.; Jia, C.; Kim, J. Aerogel nanoarchitectonics based on cellulose nanocrystals and nanofibers from eucalyptus pulp: Preparation and comparative study. *Cellulose* **2022**, *29*, 817–833. [CrossRef]
34. Zhu, Z.; Long, Y.; Xue, X.; Yin, Y.; Zhu, B.; Xu, B. Phase-transition kinetics of calcium-doped TiO_2: A high-temperature XRD study. *Ceram. Int.* **2022**, *48*, 25056–25063. [CrossRef]
35. Fan, M.; Lin, Z.; Zhang, P.; Ma, X.; Wu, K.; Liu, M.; Xiong, X. Synergistic effect of nitrogen and sulfur dual-doping endows TiO_2 with exceptional sodium storage performance. *Adv. Energy Mater.* **2021**, *11*, 2003037. [CrossRef]
36. Wang, S.; Xu, H.; Hao, T.; Wang, P.; Zhang, X.; Zhang, H.; Xue, J.; Zhao, J.; Li, Y. In situ XRD and operando spectra-electrochemical investigation of tetragonal WO3-x nanowire networks for electrochromic supercapacitors. *NPG Asia Mater.* **2021**, *13*, 51. [CrossRef]
37. Zhu, W.; Han, M.; Kim, D.; Zhang, Y.; Kwon, G.; You, J.; Jia, C.; Kim, J. Facile preparation of nanocellulose/Zn-MOF-based catalytic filter for water purification by oxidation process. *Environ. Res.* **2022**, *205*, 112417. [CrossRef]
38. Wu, L.; Chen, M.; Xu, J.; Fang, F.; Li, S.; Zhu, W. Nano-SiO_2-Modified Waterborne Acrylic Acid Resin Coating for Wood Wallboard. *Coatings* **2022**, *12*, 1453. [CrossRef]
39. Li, W.; Chen, Z.; Yu, H.; Li, J.; Liu, S. Wood-Derived Carbon Materials and Light-Emitting Materials. *Adv. Mater.* **2021**, *33*, 2000596. [CrossRef]
40. Sheng, C.; Wang, C.; Wang, H.; Jin, C.; Sun, Q.; Li, S. Self-photodegradation of formaldehyde under visible-light by solid wood modified via nanostructured Fe-doped WO_3 accompanied with superior dimensional stability. *J. Hazard. Mater.* **2017**, *328*, 127–139. [CrossRef]

41. Li, X.; Li, H.; Huang, Y.; Cao, J.; Huang, T.; Li, R.; Zhang, Q.; Lee, S.-C.; Ho, W. Exploring the photocatalytic conversion mechanism of gaseous formaldehyde degradation on TiO_{2-x}-OV surface. *J. Hazard. Mater.* **2022**, *424*, 127217. [CrossRef] [PubMed]
42. Jiang, Y.; Zhao, W.; Li, S.; Wang, S.; Fan, Y.; Wang, F.; Qiu, X.; Zhu, Y.; Zhang, Y.; Long, C. Elevating Photooxidation of Methane to Formaldehyde via TiO_2 Crystal Phase Engineering. *J. Am. Chem. Soc.* **2022**, *144*, 15977–15987. [CrossRef] [PubMed]